

Surface structure tuning in alcohol melts by bulk additives

O. Gang^{a,*}, B.M. Ocko^b, X.Z. Wu^c, E.B. Sirota^d, M. Deutsch^a

^a Department of Physics, Bar-Ilan University, Ramat-Gan 52900, Israel

^b Department of Physics, Brookhaven National Laboratory, Upton, NY 11973, USA

^c IBM Almaden Research Center, San Jose, CA 95120, USA

^d Exxon Research and Engineering Co., Annandale, NJ 08801, USA

Abstract

Surface freezing, i.e. the formation of a solid bilayer at the surface of a pure alcohol melt above the freezing temperature, was recently discovered. We demonstrate here that the structure of the bilayer can be influenced by specific bulk additives. Two different additives, able to form hydrogen bonds (water) and both hydrogen bonds and van der Waals interactions (α,ω -diols), are used. The surface layer's structure is studied by surface-specific X-ray methods. We find that water swells the bilayer by intercalation into its center at a molecular water:alcohol ratio of $\sim 1:2$. For the diolated alcohols a reversible monolayer–bilayer surface phase transition is observed, the first of its kind for surface-frozen layers. A continuous decrease of the molecular tilt with increasing diol concentration is also found for the tilted bilayer phases. © 2000 Elsevier Science B.V. All rights reserved.

Keywords: Surface freezing; Pure alcohol melts; Bulk additives; Monolayer–bilayer surface phase transition

1. Introduction

The most common surface behaviour of a solid near the melting point is that of surface melting, where the surface melts at a temperature lower than that of the bulk. The existence of a crystalline surface phase above the bulk freezing temperature, T_b , i.e. surface freezing, (denoted SF) was recently found in melts of normal-alkanes [1,2], alcohols [3,4], and several related chain compounds, as well as binary mixtures of different-length alkanes and alcohols [5,6]. Related effects were also observed on alkanes at solid substrate

surfaces [7]. In alkanes, the van der Waals (vdW) intermolecular interaction induces the formation of a crystalline monolayer at the melt's surface for a range $\Delta T \leq 3^\circ\text{C}$ above the bulk freezing point and for $15 \leq n \leq 50$. However, in alcohols ($\text{H}(\text{CH}_2)_n\text{OH}$, denoted C_nOH) a crystalline bilayer, rather than a monolayer, is formed at a temperature $T_s > T_b$, albeit with a smaller $\Delta T \leq 1^\circ\text{C}$ and $16 \leq n \leq 28$. As the only difference between the alkane and alcohol molecule is the replacement of a hydrogen by a hydroxyl on a terminal carbon, clearly the bilayer structure originates in, and is stabilized by hydrogen bonds (HB) between the alcohols' hydroxyl groups, which were found to reside at the center of the bilayer [4].

* Corresponding author.

E-mail address: mail.biu.ac.il (O. Gang)

In this study we investigate the possibility of tuning the SF effect and the structure of the surface bilayer of alcohols by varying the effective strength of the HB. This is carried out by adding small amounts of HB-forming molecules to the bulk alcohol. Two molecules, both smaller than the alcohol molecule, were of specific interest. The first is the obvious choice: water. The other is the α,ω -diol, which consists of a hydrocarbon chain with two hydroxyl groups, one at each terminal carbon. The study shows that while water intercalates into the center of the surface frozen bilayer, the hydrophobic repulsion between the alcohols' hydroxyls and the diol's alkyl chain is sufficient to prohibit such an intercalation for even the shortest diol investigated, 1,3-propanediol ($\text{OH}(\text{CH}_2)_3\text{OH}$, denoted PD). Thus, while water intercalation induces a swelling of the surface bilayer, no such swelling occurs for diols. Rather, the diol induces, presumably through varying the relevant surface energies, a concentration-dependent tilt variation in the surface bilayer's molecules, as well as a reversible monolayer–bilayer phase transition, which is driven by either temperature or diol concentration variation.

2. Experimental

The structural studies reported here employed temperature-dependent X-ray reflectivity (XR), X-ray grazing incidence diffraction (GID), and Bragg rod (BR) measurements at the free surface of alcohol melts, using synchrotron radiation at beamline X22B, NSLS, Brookhaven National Laboratory. The formation of a surface layer of an electron density, ρ_e , different from that of the bulk results in the appearance of periodic modulations in the reflectivity curve, with a period inversely proportional to the layer thickness. GID probes the structure within surface plane, and yields sharp diffraction peaks characteristic of the surface layer's in-plane crystalline structure, if present. BR, i.e. the surface-normal intensity distribution at the GID peak position, yields information on the molecular length and the magnitude and direction of the molecular tilting [8,9].

The >99% pure materials were obtained commercially, and used as received. Samples were formed by placing ~ 0.5 g of the material on a flat copper wafer inside a sealed cell, the temperature of which was regulated to $\leq 0.005^\circ\text{C}$. Hydration was done by keeping the sample under a saturated water vapor atmosphere throughout the measurement. Dilation was accomplished by direct mixing of the alcohol with the required amount of diol. Further details on the experiment and technique are given in Refs. [2,8,9].

3. Results and discussion

We now discuss the results obtained for the two additives. The hydrated alcohol results, some of which have already been published [4], are only summarized briefly, while the newer diol results are presented in more detail.

3.1. Hydrated alcohols

The existence of a surface layer of an electron density ρ_e different from the bulk yields a periodic modulation, akin to the Kiessig Fringes in Optics, in the X-ray reflectivity curves of the melts' free surfaces [8], as shown in Fig. 1a, where the reflectivity R is normalized to the Fresnel reflectivity, R_f , of an ideal surface [8]. The surface-normal electron density profiles (Fig. 1b) were obtained by computer fits (lines in Fig. 1a) of a model [2,8] representing the surface bilayer's electron density profile by five slabs: (1) top monolayer's CH_3 -group; (2) top monolayer's $(\text{CH}_2)_{n-1}$ chain; (3) the top and bottom monolayers' OH headgroups; (4) bottom monolayer's $(\text{CH}_2)_{n-1}$ chain; and (5) bottom monolayer's CH_3 -group. The thicknesses and densities of slabs 1 and 5, and of 2 and 4 were constrained to be equal. The model was convoluted with a Gaussian of a variable width representing the roughness of the surface due to thermally induced capillary waves.

The difference in the modulation period between the dry (a) and the hydrated (b) alcohol, observed in Fig. 1a, indicates a difference in the thickness of the corresponding surface frozen layers. In the model fits (lines in Fig. 1a) an increase

in the thickness of the OH slab by ~ 2.5 Å is observed for the hydrated case. The comparison in Fig. 2 of the fit results for all dry and hydrated alcohols studied demonstrates the systematic swelling of the bilayer's OH region by 2.4–2.7 Å (see the inset cartoon). Direct integration over the density profiles yields an increase of ~ 14 electrons upon hydration in a molecular area of a single chain, $A \approx 19.5$ Å². This is somewhat more than, but not too far from, the ten electrons of a single water molecule, indicating the intercalation of approximately one water molecule in between each pair of upper and lower alcohol molecules in the bilayer. This $\sim 1:2$ molecular ratio, surprisingly larger than the $\sim 1:4$ ratio in the bulk

alcohol's liquid phase, results in an almost two-fold increase in the temperature range of existence, ΔT_b , for the surface frozen layer, and for the appearance of the SF effect for $10 \leq n \leq 14$, which do not show the effect when dry.

Finally, the in-plane structure of the surface layer of the dry and the hydrated alcohol remains the same: an hexagonally packed bilayer with untilted ($n \leq 22$) or tilted ($n > 22$) molecules. A large crystalline coherence length, ≥ 1000 Å, is found for the hydrated alcohols of all n , similar to the dry, untilted, ones. A very slight decrease of the molecular tilt $\sim 1^\circ$ was detected in the Bragg rods measurements for the tilted alcohols C₂₆OH and C₂₈OH. Further details, as well as a theory accounting for the surface phase diagram by considering the surface and bulk hydration levels are given in Ref. [4].

3.2. Diolated alcohols

For the small, hydrophilic water molecule there is no energy barrier for intercalation into the center of the surface bilayer, where it forms HB bridges between the alcohol molecules and thus increases the stability of the crystalline structure both at the surface [4] and in the bulk [10]. For diols, by contrast, the hydrophobic alkyl chain results in such a barrier, effectively preventing intercalation. Thus no structural changes should be expected for the bilayer upon diolation. In practice, however, experiments reveal several dramatic structural changes induced by the diols, including the formation of a monolayer phase and variations in the molecular tilt in the bilayer phase. We now discuss these two effects in some detail.

3.2.1. Surface phases and phase transitions

3.2.1.1. The transitions. The most outstanding effect observed in these experiments is a reversible monolayer–bilayer phase transition in the surface-frozen layer, induced by varying either the temperature or the PD concentration. The transition is demonstrated in Fig. 3b, which shows the measured X-ray reflectivity off a 92%-C₂₂OH:8%PD mixture at a fixed $q_z = 0.25$

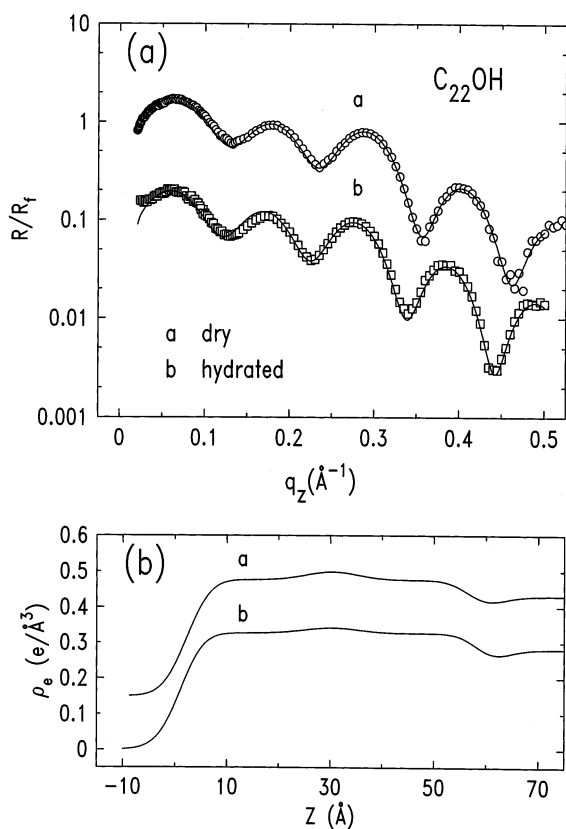


Fig. 1. (a) X-ray reflectivity R (normalized to the Fresnel reflectivity R_f of an ideal surface) of surface-frozen C₂₂OH (points), for dry and hydrated samples. Five-slab model fits (lines), discussed in the text, correspond to the surface-normal electron density profiles shown in (b). The curves are shifted for clarity.

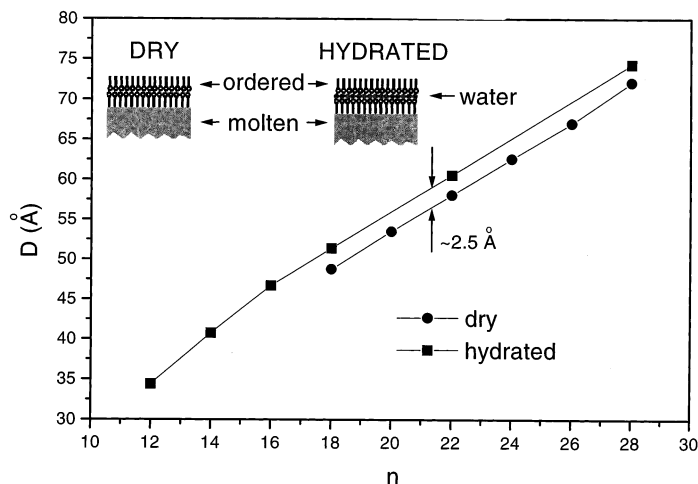


Fig. 2. The thickness of the surface bilayers obtained from the fits to the X-ray reflectivity curves. A uniform swelling by ~ 2.5 Å is observed due to water intercalations into the bilayer's center, as shown in the inset cartoons, where the vertical lines represent the alkyl chains and the circles — the OH headgroups.

Å⁻¹ as the temperature is varied. Two jumps are observed: one at $T_{s1} = 69.3^\circ\text{C}$, and the other at $T_{s2} = 68.2^\circ\text{C}$. As the full reflectivity curves taken within the regions defined by these temperatures indicate (Fig. 3a), and as discussed below, the two jumps mark transitions from a liquid to a monolayer surface phase at T_{s1} and from a monolayer to a bilayer phase at T_{s2} , respectively. The sharp jump indicates first-order transitions, at least within the $\leq 0.005^\circ\text{C}$ of our experiment. A third jump, at $T_b = 66.4^\circ\text{C}$ is due to bulk freezing, where the surface roughens macroscopically and the XR drops abruptly to near-zero.

3.2.1.2. The structure of the surface layer. Fig. 3a shows the measured, Fresnel-normalized reflectivity curves for 92% C_{22}OH :8%PD for different surface phases (a–c). The Kiessig fringes in curves a and b indicate the existence of a thin, dense surface layer. The longer modulation period, Δq_z , of b indicates a thinner layer than that of a. The monotonically decreasing curve c, measured at $T \gg T_{s1} = 69.3^\circ\text{C}$, is typical for an unstructured liquid surface.

Detailed surface-normal density profiles $\rho_e(Z)$ (Fig. 3c) were obtained by model fits to the data (lines in Fig. 3a). The electron density profile of the liquid, c, was modeled by a step-function like

density profile, smeared with a Gaussian roughness distribution at the surface [8], originating in thermally excited capillary waves [11]. Several different models were examined for the monolayer curve b. Despite the differences, the models yielded similar electron density profiles, all having an increased (relative to the bulk) electron density at the layer–liquid interface. The excess density decreases gradually from that of the OH layer to that of the bulk. This tail is poorly approximated by a step function smeared by a Gaussian. A much better approximation is a decaying exponential. Thus, the actual density model for the surface structure in the monolayer phase has three slabs: (1) the top terminal CH_3 headgroup; (2) the CH_2 chains of the monolayer; (3) the OH headgroups, plus an exponential connecting the OH box and the constant-density substrate (the bulk melt) [12]. A good quality fit was obtained for this model (line b in Fig. 3a) for that model. The electron density profile (curve b in Fig. 3c) shows the alcohol monolayer's down-pointing OH headgroups at $z \approx 30$ Å. The exponentially decaying density from this point to $z \approx 30$ Å is most probably due to a concentration of OH groups higher than that of the bulk. This, in turn, come from adsorption of both alcohol and PD molecules from the liquid to the monolayer's OH bottom

layer. Further measurements are now in progress to determine the structure of the monolayer more accurately [12].

For the bilayer phase (curve a in Fig. 3a) the same five-slab model, used for pure and hydrated alcohols (see above), was employed. The electron density profile obtained from the fit (line) to the reflectivity (curve a in Fig. 3c) indicates the same structure as that of pure alcohols. We also obtain a small increase ($< 1 \text{ \AA}$), which, however, is within the experimental uncertainty.

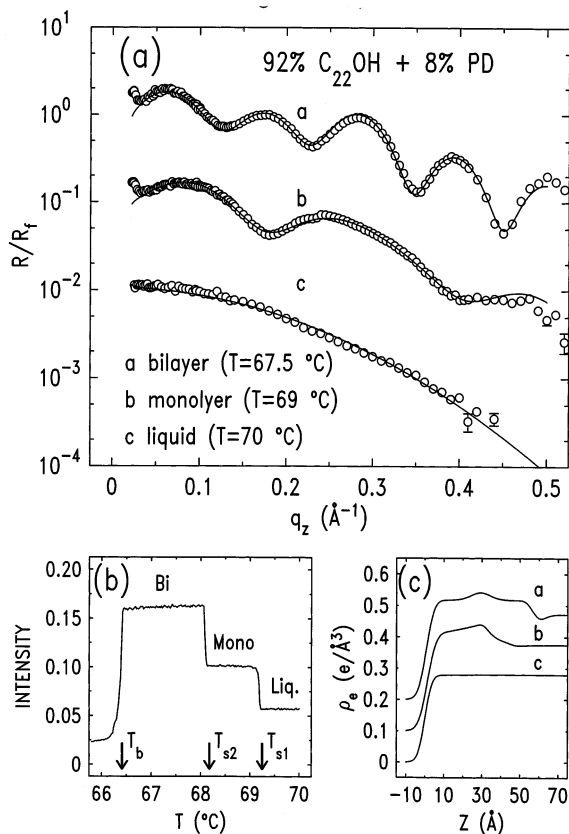


Fig. 3. (a) Normalized X-ray reflectivity off a $C_{22}OH:PD$ melt for the different temperatures, and surface phases, indicated. The lines are fits to the models discussed in the text, and correspond to the surface-normal density profiles shown in (c). (b) X-ray reflectivity at constant $q_z = 0.25 \text{ \AA}^{-1}$. The first-order liquid–monolayer (T_{s1}) and monolayer–bilayer (T_{s2}) surface phase transitions are manifested as jumps in the reflectivity. (c) Electron density profiles of a bilayer (a), monolayer (b) and liquid (c) surface phase, obtained from the fits to the reflectivity curves in (a).

The in-plane structure of both the monolayer and bilayer phases was studied by GID and BR measurements. For the monolayer phase an hexagonal, untitled molecular packing is observed. The spacing varies slightly from an intermolecular distance of 4.94 \AA for $n = 20$ to 4.87 \AA for $n = 28$, as compared to 4.83 \AA in the untitled bilayer phase of pure alcohols. For the bilayer phase of alcohol:PD mixtures with $n < 22$, where the pure material's surface-frozen phase consists of vertically oriented molecules, a slightly larger intermolecular distance of 4.90 \AA is observed for all n , relative to the 4.83 \AA of pure alcohols. No diol concentration dependence is observed in either the monolayer or the bilayer spacings for these phases [4]. However, for chain lengths $n \geq 24$, where tilted surface surface phases occur in the pure sample, a new behaviour is observed for the bilayer phase, as discussed in Section 3.2.2.

3.2.2. Tilt variation in the bilayer phase

The second novel effect observed in this study is a continuous tilt variation of the molecules in the surface-frozen tilted bilayer phases ($n \geq 24$) as the PD concentration is varied. For example, in the pure $C_{28}OH$ the surface-frozen bilayer's molecules are tilted by $\sim 20^\circ$ from the surface normal, in the next-nearest neighbor (NNN) direction. For the $(1-x)CH_{28}OH:xPD$ mixtures, the X-ray reflectivity shown in Fig. 4, reveals a continuous decrease in the period of the Kiessig fringes for $x = 7$ and 12% relative to the pure material. A five-slab model fit (lines) yields a very good agreement, and the corresponding electron density profiles (inset) show a surface bilayer with gradually increasing thickness: from 69 \AA for the pure $C_{28}OH$ to 76 \AA for $88\%C_{28}OH:12\%PD$.

GID yields two in-plane peaks at $q_{\parallel} \approx 1.44$ and 1.46 \AA^{-1} for pure $C_{28}OH$, corresponding to a distorted hexagonal packing with a molecular area $\sim 20.5 \text{ \AA}^2$. The $C_{28}OH:PD$ mixtures also show the same two-peak GID pattern. However, the splitting varies with PD concentration x . For $x = 7\%$ the peaks are at $q_{\parallel} \approx 1.48$ and 1.49 \AA^{-1} , while for $x = 12\%$ they are at $q_{\parallel} \approx 1.49$ and 1.50 \AA^{-1} . The lowest-order BR corresponding to the GID peaks are shown for each concentration in Fig. 5a. They are typical of NNN tilted molecules

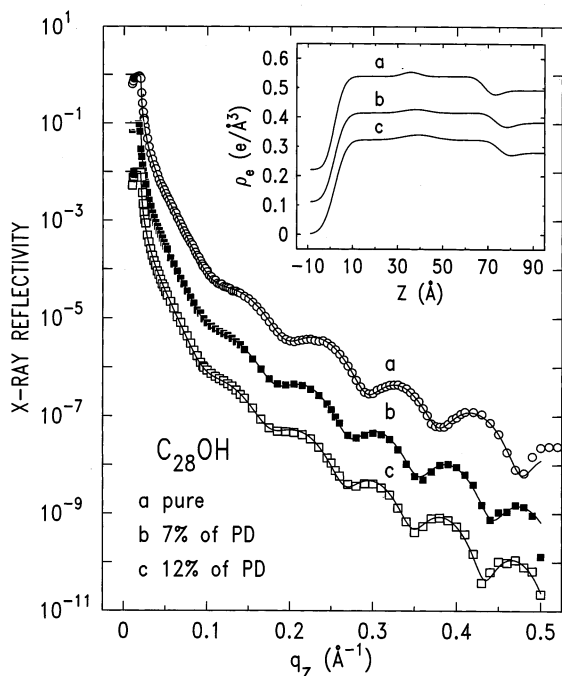


Fig. 4. X-ray reflectivity of surface-frozen $C_{28}OH:PD$ for different concentrations (points). Five-slab model fits are shown in lines, and the corresponding electron density profiles are given in the inset. The decrease in the modulation period with increasing PD concentration indicates a corresponding increase in the bilayer's thickness.

[4,12]. The BR peak positions $q_z = 0.24 \text{ \AA}^{-1}$ (pure), $q_z = 0.19 \text{ \AA}^{-1}$ (7% PD) and $q_z = 0.15 \text{ \AA}^{-1}$ (12% PD), indicate considerably different tilt angles. A full-curve fit (lines) yields $\sim 20^\circ$ for the pure sample, and $\sim 17^\circ$ and $\sim 13^\circ$ for the $93\%C_{28}OH:7\%PD$ and $88\%C_{28}OH:12\%PD$, correspondingly, as shown in Fig. 5b. These values account in full for the thickness variations observed in the XR measurements discussed above. This, in turn, indicates that no layer swelling, and thus no intercalation of PD molecules into the bilayer, occurs here in contrast with the swelling observed for hydrated alcohols. As discussed above, this difference is expected in view of the hydrophobicity of the PD's alkyl chain. The tilt variations are driven, therefore, by the variation in the hydrophilicity of the subphase due to changes in the OH-rich PD concentration. This change varies the bilayer–subphase interaction,

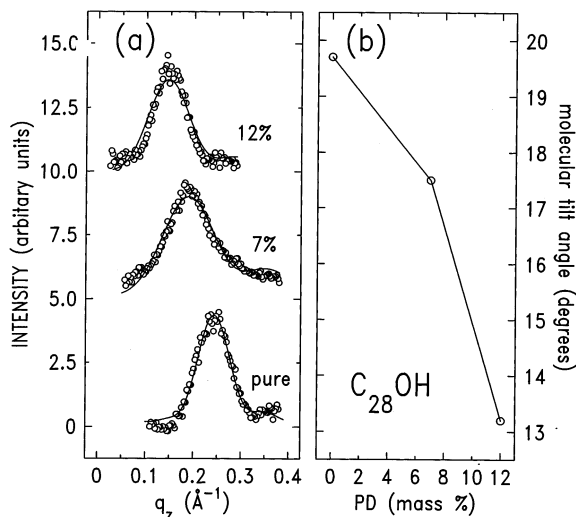


Fig. 5. (a) Bragg rods of the surface-frozen bilayers of $C_{28}OH$ for different PD concentrations. The shift of the peak from $q_z = 0.24 \text{ \AA}^{-1}$ for pure material to $q_z = 0.19$ and $q_z = 0.15 \text{ \AA}^{-1}$ for the $93\%C_{28}OH:7\%PD$ and $88\%C_{28}OH:12\%PD$ indicates a decrease in the molecular tilt. The lines are model fits. (b) Molecular tilt angles derived from the fits. A clear decrease in tilt with increasing PD concentration is observed.

leaving the other two dominant interactions, the in-plane chain–chain interaction and the hydrogen bonding of the two layers unchanged. The variation in the balance between these interactions varies the tilt. Other structural characteristics, dominated by the same interactions, are less sensitive to these variations and are influenced only little (spacing) or not at all (the hexagonal packing).

4. Conclusions

The role of hydrogen bonding between alcohol and the additive molecules in the surface-frozen layer was studied. Although the surface behavior of the system mainly depends on the alcohol properties, the different nature of the additive molecules results in a different influence on the structure of the surface layer. This is reflected, for example, in the fact that hydration increases the bulk and surface melting temperatures, while dioilation reduces them. This indicates that the water molecule increases the stability of the crystalline

phase, while the diol reduces it. Corresponding differences are found in the molecular-level structure of the surface layer. The intercalation of water molecules into OH region of the surface-frozen alcohol bilayer, with a molecular alcohol:water ratio $\sim 2:1$, caused a swelling by about 2.5 Å. The 1,3-propanediol molecules, due to their hydrophobic alkyl chain, do not penetrate into bilayer. However, by changing the bilayer–liquid interfacial energy, they change the molecular tilt in the bilayer commensurately with the concentration. This is an exclusive surface effect for which no parallel bulk behavior was observed [12]. The difference is due, most probably, to the fact that the 3D crystal structure excludes the diol molecules, so that no close contact is possible between the ordered alcohols and the diols. However, in the case of a crystalline surface layer on top of a liquid melt the diol molecules dissolved in the melt can approach the crystalline layer close enough to influence the tilt. Finally, the appearance of a new monolayer surface phase, having, again, no parallel in the bulk phases, was also observed, and its structure studied. These results indicate that molecular level engineering of the surface-frozen layer's structure by bulk additives is a viable prospect, which may have important implications for future practical applications.

Acknowledgements

The financial support of the work at Bar-Ilan University by Exxon Research and Engineering

Co. is gratefully acknowledged, as is the beam-time allocation at beamline X22B, NSLS, BNL. Brookhaven National Laboratory is supported by the division of Materials Research, DOE, under contract DEAC02-98CH10886.

References

- [1] (a) X.Z. Wu, E.B. Sirota, S.K. Sinha, B.M. Ocko, M. Deutsch, *Phys. Rev. Lett.* 70 (1993) 958. (b) X.Z. Wu, B.M. Ocko, E.B. Sirota, S.K. Sinha, M. Deutsch, G.H. Cao, M.W. Kim, *Science* 261 (1993) 1018.
- [2] B.M. Ocko, X.Z. Wu, E.B. Sirota, S.K. Sinha, O. Gang, M. Deutsch, *Phys. Rev. E* 55 (1997) 3164.
- [3] M. Deutsch, X.Z. Wu, E.B. Sirota, S.K. Sinha, B.M. Ocko, O.M. Magnussen, *Europhys. Lett.* 30 (1995) 283.
- [4] (a) O. Gang, B.M. Ocko, X.Z. Wu, E.B. Sirota, M. Deutsch, *Phys. Rev. Lett.* 80 (1998) 1264. (b) O. Gang, X.Z. Wu, B.M. Ocko, E.B. Sirota, M. Deutsch, *Phys. Rev. E* 58 (1998) 6068.
- [5] X.Z. Wu, B.M. Ocko, H. Tang, E.B. Sirota, S.K. Sinha, M. Deutsch, *Phys. Rev. Lett.* 75 (1995) 1332.
- [6] X.Z. Wu, A. Doerr, B.M. Ocko, E.B. Sirota, O. Gang, M. Deutsch, *Coll. Surf. A* 128 (1997) 63.
- [7] C. Merkl, T. Pfohl, H. Riegler, *Phys. Rev. Lett.* 79 (1997) 4625.
- [8] (a) M. Deutsch, B.M. Ocko, in: G.L. Trigg (Ed.), *X-ray and Neutron Reflectivity in Encyclopedia of Applied Physics*, vol. 23, VCH, New-York, 1998. (b) T.P. Russell, *Mater. Sci. Rep.* 5 (1990) 171.
- [9] J. Als-Nielsen, K. Kjær, in: T. Riste, D. Sherrington (Eds.), *Phase Transitions in Soft Condensed Matter*, Plenum, New York, 1989.
- [10] E.B. Sirota, X.Z. Wu, *J. Chem. Phys.* 105 (1996) 7763.
- [11] B.M. Ocko, X.Z. Wu, E.B. Sirota, S.K. Sinha, M. Deutsch, *Phys. Rev. Lett.* 72 (1994) 242.
- [12] O. Gang et al. (submitted).